

# PROTOTYPE DEVELOPMENT OF A COMPACT HTS WIGGLER FOR SYNCHROTRON LIGHT SOURCES

L. Bortot\*, C. Benabderrahmane, F. Cianciosi, G. Le Bec, F. Perratone, Z. Qiu  
European Synchrotron Radiation Facility, Grenoble, France

## Abstract

The European Synchrotron Radiation Facility is developing a novel, compact, superconducting wiggler for beamline BM18. The design features three pole pairs delivering up to 1.58 T at 60 K using high-temperature superconducting tapes and a no-insulation winding technique. A current-controlled continuous field variation ensures field-tunability requirements for low-photon energy applications within tight space constraints. Completed milestones include magnetic and thermal design, HTS tape procurement, and winding prototype testing. A production winding machine will be delivered in May 2026, followed by the wiggler assembly. Upcoming 77 K testing will validate the wiggler before final installation.

## INTRODUCTION

The European Synchrotron Radiation Facility (ESRF) is pursuing the development of short-period, high-field, high-temperature superconducting (HTS) undulators for future synchrotron radiation sources [8]. In this framework, a field-tunable HTS wiggler is currently being developed for beamline BM18 upgrade to enable low-photon energy applications. In conventional permanent-magnet wigglers, such tunability relies on mechanical gap variation, which is impractical within the severe spatial constraints. This HTS wiggler serves dual purposes: as a demonstrator for BM18 and as a technological development platform for future HTS undulators.

This paper presents the wiggler design, manufacturing progress, and preparations for prototype validation. Design criteria emphasize simplicity and robustness to minimize technical risk while ensuring reliable operation for user experiments. The project builds on ESRF's 30-year legacy [5] and serves as a technological development platform for future short-period, high-field HTS undulators.

## MAGNET DESIGN

The magnet assembly has dimensions of 200 mm in length, 90 mm in width, and 120 mm in height. The magnet features an iron-dominated configuration with rectangular-like coils wound on magnetic poles made of pure iron, producing a peak field of 1.58 T in a magnetic gap of 24 mm at 60 K. The magnet vacuum is separated from that of the storage ring. The complete wiggler is shown in Fig. 1. The iron yoke serves both as magnetic flux circuit and structural support for the windings and the titanium brackets that withstand the electromagnetic vertical forces during operation,

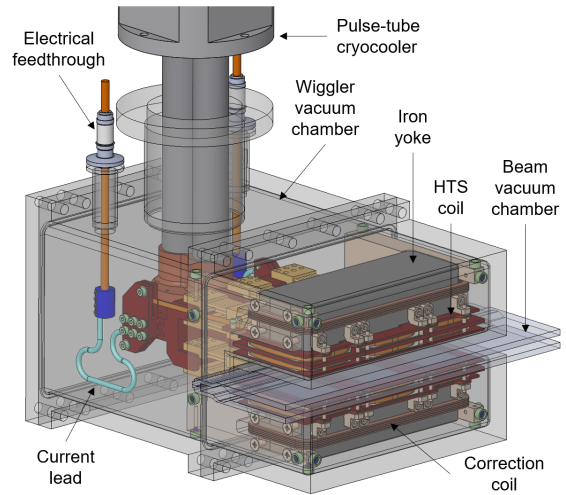


Figure 1: HTS superconducting wiggler including the magnet assembly, the cryocooler cold head, and the vacuum chamber.

up to 5 kN. The main design parameters of the magnet are summarized in Table 1.

Table 1: Specifications of the Superconducting Wiggler

Parameter	Unit	Value
Magnetic gap	mm	24
Maximum field strength	T	1.58
Peak field at conductor	T	1.5
Operating temperature	K	60
Field integral target	T mm	<0.1
Field integral tunability	T mm	$\pm 0.5$
Operating current	A	80
Quench margin	%	35
Inductance	mH	38
Stored energy	kJ	0.125

The superconducting coil consists of three pole pairs. The coil is wound using rare-earth barium-copper-oxide (REBCO) HTS tapes. The tapes feature a critical current of 120 A at 77 K in self field conditions. The coil comprises six double-pancake windings: the central pole pair features 113 turns per pancake, while each side pole pair contains 53 turns. At nominal current of 80 A, this configuration provides a total excitation of 72 kA t, for a stored magnetic energy of 0.125 kJ and an inductance of 38 mH. The magnetic field profile and the residual of the first field integral are shown in Fig. 2. The latter is kept below 0.1 T mm across the operating current range. To address residual field errors, the magnet assembly is equipped with a correction coil made

\* lorenzo.bortot@esrf.fr

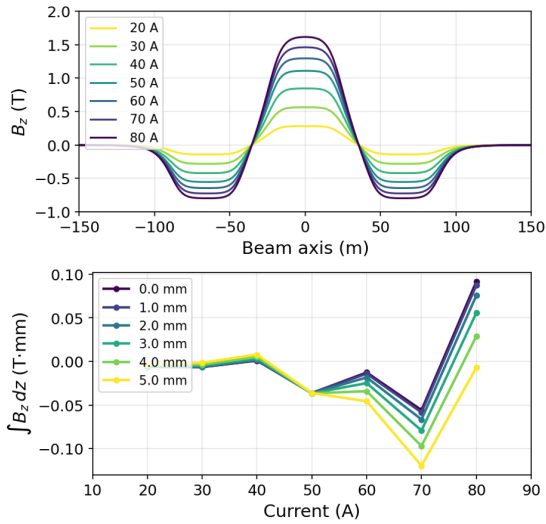


Figure 2: Magnetic field profile as a function of current (top). Residual field error as function of current and beam displacement (bottom).

of copper wire, capable of providing up to  $\pm 0.5$  T mm of tunable field integral.

The interlayer electrical contact between pancakes is provided by the copper mandrel on which the coil is wound. The inter-pole contact is achieved through demountable joints to enhance modularity and simplify assembly and maintenance. The design of the winding demountable joints features the use of copper blocks with indium inserts [10] that are preloaded against the coil by springs.

The coil is operated with a quench margin of 35%. Windings are dry-wound according to the no-insulation (NI) technique [9]. This allows for current redistribution between turns during quench events, enhancing the self-protecting behavior [6]. This mechanism is particularly effective for small coils with low stored energy, where energy spread is rapid enough to prevent local hot spots.

### Field Optimization

The iron yoke shape was optimized to minimize first and second field integrals over the operating current range. This was achieved by applying a stochastic optimization to the wiggler model developed in RADIA [2]. The optimization runs in parallel on the ESRF HPC cluster. The residual field errors are reduced to less than 0.1 T mm for the first integral. Residual errors are compensated by the correction coils.

The quench margin was verified through a 3D model developed in COMSOL Multiphysics, ensuring the optimized geometry operates within safe thermal margins at the 60 K operating temperature. Critical current measurements at 77 K from the tape supplier were scaled using the lift factor from the HTS critical current database [3, 4].

## CRYOGENIC DESIGN

The cryostat vessel consists of a rectangular vacuum chamber made of a non-magnetic metal, with the material selection currently under evaluation. It houses the magnet assembly,

electrical feedthroughs, current leads and the cryocooler which maintains the operating temperature below 60 K. The vessel is composed of two halves bolted together, with a removable lid on one side for access and inspection of the magnet assembly. The vessel half containing the magnet cold mass has a C-shape design. This design allows for easy installation and removal of the magnet assembly for maintenance and in case of failure, without compromising the vacuum integrity of the storage ring.

The vessel thickness is limited to 2 mm at the magnetic poles, representing a compromise between deformation from vacuum pressure and minimizing the pole-to-pole distance. A primary vacuum below 1 mbar is maintained by a primary pump. The cryostat design incorporates up to ten layers of multi-layer insulation (MLI) [12] between the cold mass including the current leads and the vacuum vessel. The magnet gap region is excluded from MLI coverage, at the cost of higher thermal losses, to minimize the distance between the magnet poles.

The magnet assembly is insulated from the vacuum vessel by low thermal conductivity fiberglass posts, which also provide mechanical support and alignment. The current leads operate between 60 K and 300 K and are thermally anchored to the cold head through copper braids. The current leads are designed following [11] as conduction-cooled type made of copper with low thermal conductivity ( $RRR < 50$ ) and can carry up to a maximum current of 100 A.

The cooling system is a single-stage, pulse-tube cryocooler with a capacity of 60 W at 60 K, and commercially available as PT90 from Cryomech. Conduction cooling was selected to simplify operation and maintenance while reducing operational costs compared to liquid-cryogen systems and infrastructure. The cold head is linked to the coil mandrels via copper braids to provide mechanical decoupling and minimize vibrations that could affect beam stability. Coil windings are conduction-cooled through their corresponding copper mandrels, whereas aluminum nitride interfaces located between the NI coil and the cold head provide high thermal conductivity and high electrical insulation.

### Thermal Budget

A simplified zero-dimensional thermal design was used to estimate the expected heat loads and cooling requirements under conservative assumptions for a peak current of 100 A. Results guided the detailed magnet design, and subsequent 3D thermal simulations verified the conduction-cooling performance.

The total heat load on the magnet assembly is estimated at approximately 32 W at 60 K. Contributions are summarized in Table 2. Heat load is dominated by current leads (13 W) and radiative load (12 W, calculated without MLI as a conservative assumption). Thermal losses in coil joints, correction coils, and support posts are minor contributions and are also included (Table 2). The estimated heat load is well within the cooling capacity of 60 W at 60 K for the selected cryocooler, providing a conservative safety margin of about 1.8 for operation.

Table 2: Thermal Loads at 60 K for the Magnet Assembly

Quantity	Unit	Value
Radiative load	W	12.0
Current leads	W	13.0
Coil joints	W	1.5
Correction coil	W	2.0
Support posts	W	2.0
Beam chamber	W	1.5
Total heat load	W	32.0

## MANUFACTURING AND WINDING

Winding tests were conducted using an experimental winding machine built in-house to understand HTS tape behavior and de-risk final-scale manufacturing. The approach follows a rapid iteration and continuous improvement philosophy, reducing development time. Initial designs assumed a filleted rectangle mandrel geometry for simplicity, but this configuration revealed critical issues: poor tape-to-mandrel contact and excessive stress concentrations in the fillets.

Through experimental optimization, we replaced a fraction of straight sections with circular arcs having continuous tangents, resulting in a rectangular-like shape where straight sections are partially replaced by circular arcs. This design provides excellent tape-to-mandrel contact and significantly reduces stress concentrations in the corner regions, as shown in Fig. 3.

### Winding Machine Specifications

A fully automated roll-to-roll winding machine has been developed to manufacture planar HTS coils for R&D on short-period undulators. The machine supports race-track, rectangular, D-shaped, and circular coil geometries with principal dimensions ranging from 6 mm × 10 mm to 250 mm × 250 mm, covering needs for both undulators and wigglers. It features two modular pay-off units operating in forward or reverse with independent control, capable of co-winding ReBCO tape of 2-12 mm width with a second tape material.

Tension is precisely controlled within  $\pm 5\%$  in the 1-15 N range with position accuracy of  $\pm 0.1$  mm, tackling the non-trivial challenge of low-tension winding combined with tight control. These requirements were driven by the need to wind 25  $\mu\text{m}$ -thin substrate tapes for small coil dimensions (tens of mm) and small bending radii (few mm), without degrading the superconducting properties of the tape [1, 7].

The prototype control loop was designed, built, and finally tested in February 2026. The production machine is scheduled for delivery in May 2026, with full commissioning to follow immediately.

## STATUS AND NEXT STEPS

As of May 2026, the project has completed magnetic design, thermal analysis, HTS tape procurement, and winding machine prototype testing. Warm winding tests validated the arc-based mandrel geometry, improving tape-to-mandrel



Figure 3: Tape tensioning test. Left: initial filleted rectangle mandrel. Right: optimized multi-arc mandrel geometry with improved contact and reduced stress concentrations.

contact and reducing stress concentrations in corner regions. The production winding machine is scheduled for delivery in late May 2026. The immediate next steps include coil manufacturing using the production machine, followed by 77 K prototype testing to validate the current-controlled field design, then cryostat assembly and full thermal and magnetic characterization at 60 K. Field integral verification and design validation for synchrotron operation integration will follow.

## CONCLUSION

The ESRF HTS wiggler development has achieved significant progress in design and preparation phases. The magnetic design is complete, ensuring a quench margin of 35% at 60 K. The cryocooler has been identified for operations, achieving a safety margin of 1.8, and HTS tape has been procured. Warm winding tests improved mandrel geometry, transitioning to an arc-based shape that improves tape contact and reduces stress. Demountable joints have been designed to enable modular maintenance. The simple, robust, and feasible design philosophy has guided all development decisions.

The production winding machine will be delivered in May 2026, enabling coil manufacturing. Subsequent 77 K and 60 K testing will validate the current-controlled field design. This compact HTS wiggler addresses the needs of beamline BM18 for wide field tunability within tight space constraints, while serving as a technological platform toward high field, short-period HTS undulators.

## ACKNOWLEDGEMENTS

The authors thank P. Tafforeau, B. Pelissier, L. Eybert, and F. Villar for technical discussions on the magnetic, thermal, and mechanical design of the HTS wiggler.

## REFERENCES

- [1] K. Osamura *et al.*, "Reversible stress and strain limits of the critical current of practical REBCO and BSCCO wires", *Supercond. Sci. Technol.*, vol. 29, no. 9, p. 094003, 2016. [doi:10.1088/0953-2048/29/9/094003](https://doi.org/10.1088/0953-2048/29/9/094003)

- [2] O. Chubar, P. Elleaume, and J. Chavanne, "A three-dimensional magnetostatics computer code for insertion devices", *J. Synchrotron Radiat.*, vol. 5, no. 3, pp. 481–484, 1998. doi:10.1107/S0909049597013502
- [3] S. C. Wimbush and N. M. Strickland, "A public database of high-temperature superconductor critical current data", *IEEE Trans. Appl. Supercond.*, vol. 27, no. 4, pp. 1–5, Jun. 2017. doi:10.1109/TASC.2016.2628700
- [4] "Robinson HTS Critical Current Database", <https://htsdb.wimbush.eu>, Accessed: May 2026.
- [5] M. Stampfer and P. Elleaume, "A 4T Superconducting Wiggler for the ESRF", in *Proc. EPAC'94*, London, UK, Jun.-Jul. 1994, pp. 2316–2319.
- [6] J.-B. Song *et al.*, "Over-current quench test and self-protecting behavior of a 7 T/78 mm multi-width no-insulation REBCO magnet at 4.2 K", *Supercond. Sci. Technol.*, vol. 28, no. 11, p. 114001, Sep. 2015. doi:10.1088/0953-2048/28/11/114001
- [7] A. Usoskin *et al.*, "Long HTS Tapes With High In-Field Performance Manufactured via Multibeam PLD With Dynamic Drum Concept", *IEEE Trans. Appl. Supercond.*, vol. 27, no. 4, pp. 6600605, Jun. 2017. doi:10.1109/TASC.2016.2627799
- [8] K. Zhang and M. Calvi, "Review and prospects of world-wide superconducting undulator development for synchrotrons and FELs", *Supercond. Sci. Technol.*, vol. 35, no. 9, 093001, Jul. 2022. doi:10.1088/1361-6668/ac782a
- [9] S. Hahn, D. K. Park, J. Bascunan, and Y. Iwasa, "HTS pancake coils without turn-to-turn insulation", *IEEE Trans. Appl. Supercond.*, vol. 21, no. 3, pp. 1592–1595, Dec. 2010. doi:10.1109/TASC.2010.2093492
- [10] R. Hayasaka, S. Ito, T. Kato, D. Yokoe, and H. Hashizume, "In-depth resistance analysis of REBCO tape joints with indium insert and solders", in *J. Phys.: Conf. Ser.*, vol. 1559, no. 1, 012034, 2020. doi:10.1088/1742-6596/1559/1/012034
- [11] M. N. Wilson, *Superconducting Magnets*, Clarendon Press, Oxford, 1983.
- [12] P. M. Suteesh and A. Chollackal, "Thermal performance of multilayer insulation: a review", in *IOP Conf. Ser.: Mater. Sci. Eng.*, vol. 396, no. 1, 012061, 2018. doi:10.1088/1757-899X/396/1/012061